

Photon-stimulated desorption and ultraviolet photoemission spectroscopic study of the interaction of H₂O with a Ti(001) surface

Roger Stockbauer, David M. Hanson,* S. Anders Flodström,[†] and Theodore E. Madey

National Bureau of Standards, Washington, D. C. 20234

(Received 28 January 1982)

The adsorption of H₂O on a stepped Ti(001) single crystal, oriented within 4° of Ti(001) has been studied using synchrotron radiation from the Synchrotron Ultraviolet Radiation Facility at National Bureau of Standards. The species formed upon adsorption of H₂O were identified through variable-wavelength ultraviolet photoemission spectroscopy. At room temperature (~300 K), water dissociates to form O, H, and OH. At low temperature (~90 K) and low coverage (< 1 L), the same species were observed. Photon-stimulated-desorption experiments were performed under these conditions yielding predominately H⁺ ions with little or no OH⁺ or O⁺. At 90 K and coverages greater than 1 L, an ice overlayer was formed suppressing the H⁺-ion desorption. Separate experiments involving the adsorption of hydrogen and coadsorption of oxygen and hydrogen showed an order of magnitude less H⁺ desorption, indicating that the H⁺ desorption was associated with the presence of OH on the surface. The H⁺-ion yield as a function of photon energy showed a threshold at 25 eV perhaps due to O 2s excitation. A second threshold at 33 eV, a broad peak near 45 eV, and a slow decrease toward higher photon energy suggests a correlation with the Ti 3p core-hole excitation although other possibilities cannot be eliminated. Possible bonding configurations are proposed to explain the origins of the H⁺ emission.

INTRODUCTION

Water adsorbed on various substrates has been the subject of a number of recent studies. This is due in part to the importance of adsorbed water in a variety of chemical processes such as heterogeneous catalysis, electrolysis, and formation of aerosols on metal particulates. Water undergoes several possible reactions on a metal surfaces. It can adsorb dissociatively or molecularly. Early ultraviolet photoemission spectroscopy (UPS) studies of Atkinson *et al.*¹ suggested that water adsorbed on Mo dissociates. Fisher, Gland, and Sexton² determined that OH was formed on Pt(111) when water was co-adsorbed with O at low temperature and allowed to warm up. They observed a Pt-O-H scissors vibration in electron-energy-loss spectroscopy (EELS) which showed the proper frequency shift upon deuterium substitution. They obtained a UPS spectra of this species under the same conditions. Also using EELS, Ibach and Lehwald³ saw evidence for free OH and H after the adsorption of H₂O on Pt(100). Water was found to react strongly with Fe(001) by Dwyer *et al.*⁴ using low-energy electron diffraction (LEED) and Auger electron spectroscopy (AES).

Benndorf *et al.*,⁵ with the use of UPS, saw evidence for molecular H₂O adsorption on Ni(110) at low temperature followed by the formation of an ice overlayer at high coverages. On this substrate, water apparently can lose one or both of its hydrogen atoms. Recently, Rosenberg *et al.*⁶ studied the photon-stimulated desorption (PSD) of ions from amorphous ice. The only ion species they observed in the photon energy 20–35 eV was H⁺; contributions from any higher-mass ions were 3 orders of magnitude less intense. Netzer and Madey⁷ have studied the electron-stimulated desorption (ESD) of H₂O on Ni(111) and found the dominant ion to be H⁺ from fractional H₂O monolayers, as well as from adsorbed OH.

In this paper, we report evidence that H₂O dissociates on a stepped Ti(001) surface at room temperature to form H, O, and OH. The evidence is provided by variable-wavelength UPS with the identification of the species made by comparing the results of Fisher, Gland, and Sexton² for OH on Pt, the results of Feibelman *et al.*⁸ for H, and our own results⁹ for O. The dominant ion observed here in PSD from the dissociated H₂O is H⁺, which appears to be associated with the presence of the OH species bonded on the surface in at least two distinct configurations.

EXPERIMENT

The experiments were performed with the ultrahigh-vacuum instrument described previously⁹ attached to the Synchrotron Ultraviolet Radiation Facility (SURF) of the National Bureau of Standards. Two monochromators were used in these studies. The first, a grazing-incidence toroidal grating instrument with usable photon intensity from 25 to 75 eV delivered a peak flux at 50 eV of $\sim 10^9$ photons/sec on the sample. The second, a high-flux normal-incidence monochromator with a mirror-grating combination that provided usable photon intensity from 10 to 30 eV delivered a peak flux at 20 eV of $\sim 2 \times 10^9$ photons/sec on the sample¹⁰ with a current of 10 mA stored in the ring. The photons entered the UHV chamber through a reentrant exit slit on the grazing-incidence monochromator or a 2-mm i.d. capillary light pipe on the normal-incidence monochromator.¹¹ The effective exit slit in both cases was approximately 2 cm from the sample producing a 1-mm-high \times 2-mm-wide spot from the grazing incidence and a 2-mm-diameter spot from the normal incidence.

The experimental chamber was of stainless steel design with a base pressure of typically 1×10^{-10} Torr. A double-pass cylindrical mirror analyzer (CMA) was used for both the electron and ion analysis. A coaxial electron gun allowed Auger analysis of the electrons for preliminary checks of sample cleanliness and ESD ion-mass determination using a pulsed time-of-flight (TOF) technique.¹² The axis of the CMA was perpendicular to the photon beam and the crystal normal was usually 45° from the CMA axis. This configuration resulted in a mixed *s*- and *p*-photon polarization on the sample with detection of emission normal to the surface. The combined sensitivity of the photon monochromators and CMA was ~ 1 count/sec corresponding to a PSD yield of $\sim 10^{-9}$ ions/photon. The lack of a detectable PSD signal then means that the ion yield is equal to or less than $\sim 10^{-10}$ ions/photon.

Ancillary equipment in the chamber included a calibrated photodiode¹³ for monitoring the absolute photon intensity, a quadrupole mass spectrometer for residual gas analysis, and an electron gun with associated grid and microchannel plate assembly used for both LEED to observe crystal order and for electron-stimulated desorption ion angular distribution¹⁴ (ESDIAD) measurements.

The Ti(001) crystal, its preparation, cleaning, and cooling were described previously.⁹ However, we repeat here that the crystal used for the majori-

ty of this work had been cut at an angle of approximately 4° to the (001) face for other experiments and therefore represents a stepped crystal with predominantly (001) terraces. For one experiment (cf. Fig. 6 and accompanying discussion) a Ti crystal having its surface oriented within 0.5° of (001) was used.

RESULTS

Ultraviolet photoemission spectroscopy

The identification of the species present on the Ti(001) surface after H₂O adsorption is made via UPS. The spectra are shown in Fig. 1 for adsorption at room temperature (~ 300 K). At a photon energy of 23.0 eV, a 1.3-eV binding energy (BE) feature appears fully resolved from the Ti 3*d* valence band (Fig. 1, curves *b* and *c*). At higher photon energies, the cross section of the 1.3-eV peak appears to increase relative to that of the valence peak and the photon-energy resolution degrades to such an extent that the peaks are no

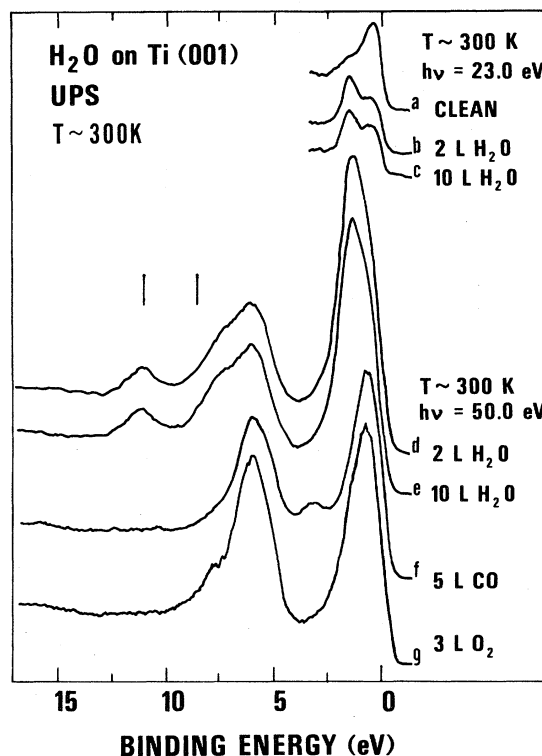


FIG. 1. UPS of water (*a*–*e*) at room temperature compared with CO (*f*) and O₂ (*g*). Curves *a*–*c* show H-induced surface state. The positions of the OH gas-phase PES peaks (Ref. 17) are shown above curve *d*.

longer resolved (see Fig. 1, curves *d* and *e*). This feature is identical in form and photon-energy dependence to the 1.3-eV BE peak observed when this same crystal was dosed with hydrogen.¹⁵ It has been identified by Feibelman *et al.*⁸ as a H-induced surface state on Ti(001). A broad peak near 6 eV observed in the hydrogen-adsorption experiments was obscured in the H₂O experiment by other peaks in the spectrum. A comparison of the relative intensities of the peaks at 6 and 1.3 eV in the H₂O and the H spectra shows that the intensity of the 6-eV peak in the H₂O spectra is a factor of 2 higher than in the H spectra, indicating an additional contribution to the 6-eV peak in the H₂O spectra.

The main contribution to the peak at 6 eV is assumed to be from atomic oxygen. This conclusion is based on previous UPS results from oxygen adsorption on the same crystal⁹ and on Ti films.¹⁶ The relative intensity of this peak compared to the peaks at 1.3, 7.4, and 11.4 eV BE is too high to be due to OH or H alone.

The peaks at 7.4 and 11.4 eV BE are ascribed to OH based on their similarity to the peaks observed by Fisher, Gland, and Sexton² in UPS of oxygen and water coadsorption on Pt(111). They identified these peaks as OH features using results from high-resolution EELS. In our UPS spectra, one might be tempted to assign these peaks to impurity CO adsorbed on the surface. Two observations rule against this possibility. First, molecular CO adsorbs dissociatively on this surface at room temperature¹⁵ producing the spectrum shown in curve *f* of Fig. 1. The peaks near 4 and 6 eV BE are due to atomic C and O, respectively. At low temperatures (90 K) CO does adsorb molecularly producing peaks at 7.3 and 11.5 eV BE, close to those observed here (see curve *b* of Fig. 3 and the discussion below). This raises the possibility that impurity CO might not dissociate in the presence of H₂O on the surface. The second observation refutes this possibility. The photon-energy dependence of the cross section of the 11.4-eV peak in the H₂O adsorption experiments is different from that of the 11.5-eV peak in the low-temperature CO adsorption as shown in Fig. 2. There are quantitative differences between the 7.4-eV OH peak and the 7.3-eV CO peak as well, even though their functional forms are similar. At photon energies in excess of 50 eV, the two peaks observed when H₂O is adsorbed have approximately equal intensities while in the CO data, the 11.5-eV peak is a factor of 4 lower than the 7.3-eV peak. Also, at photon energies below 40 eV, the peaks near 11 eV show

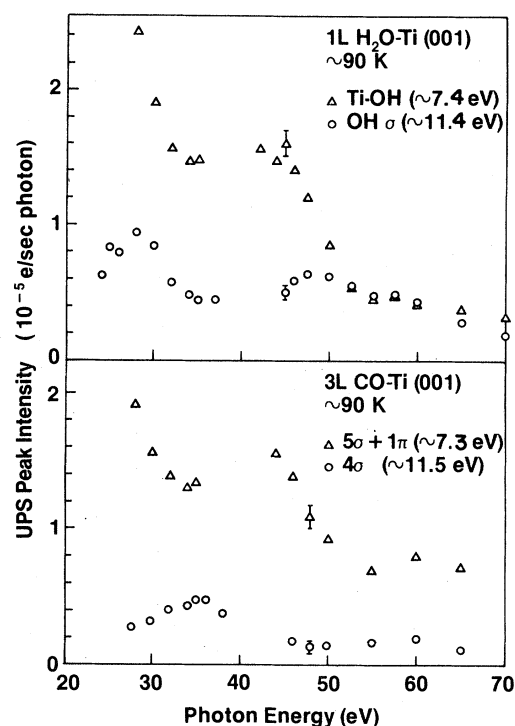


FIG. 2. Cross sections of the 7.3- and 11.4-eV UPS peaks of water on Ti(001) compared with those of CO. The gap in the data around 40 eV is due to a Ti Auger feature in this energy range.

different cross-section dependence for the two adsorbates. Based on this evidence we assert that the two peaks are due to the formation of OH when H₂O is adsorbed on Ti(001).

A comparison can be made with the UPS spectrum of gaseous OH radical which exhibits two dominant features with ionization potentials of 13.0 and 15.2 eV.¹⁷ The location of the gaseous peaks are indicated by the lines above curve *d* on Fig. 1, aligned by matching the energy of the gas-phase peak of higher ionization potential with the surface OH peak at 11.4 eV. We note that the energy spacings of gaseous OH and surface OH are different, presumably due to bonding of OH to the Ti surface.

It should be noted that the UPS data show no evidence for molecular H₂O on the surface at room temperature. As will be shown below, its presence is indicated by peaks at 8, 9–13, and 14 eV BE. No peak at 14 eV appears in any of the 300-K spectra obtained over the range of coverages investigated here, indicating the absence of H₂O at room temperature.

At low temperature (~90 K) and low coverage (< 1-L exposure), the UPS spectra show the same features as the room-temperature spectra. This is

shown in curves *c* and *d* of Fig. 3. Again, peaks are noted for H at 1.3 eV, for O at 6 eV, and for OH at 7.4 and 11.4 eV BE. As in the room temperature spectra, the H₂O appears to be fully dissociated.

At higher coverages, additional features appear: peaks at 8 and 14 eV and a plateau between 9 and 13 eV BE. Their similarity to peaks observed at low temperature by Brundle and Roberts¹⁸ from H₂O on Au, by Fisher, Gland, and Sexton² from H₂O on Pt(111), and by Benndorf *et al.*⁵ from H₂O on Ni(110) leads us to assign these features to molecular H₂O on the Ti(001) surface. In addition, the peaks have energy spacings similar to the spacings in the gas-phase photoelectron spectra¹⁹ marked at the bottom of Fig. 3. The suppression of the room-temperature features including the Ti valence peak, suggests the formation of an H₂O ice overlayer at higher coverages (see curve *f* of Fig. 3).

For comparison, the low-temperature UPS data for CO on Ti(001) is shown in curve *b* of Fig. 3. Along with the peaks observed at room temperature, however, we now observe additional peaks at 7.3 and 11.5 eV. As mentioned above and shown

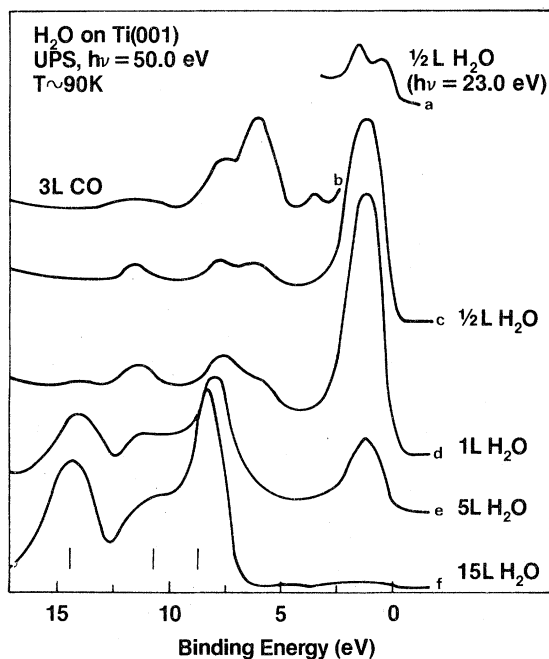


FIG. 3. UPS of water-dosed Ti(001) for different coverages at ~ 90 K compared with CO (*b*). Low coverage (*c*) shows only H, O, and OH. At higher coverages (*d*–*f*), peaks corresponding to molecular water appear. The energy of the H₂O gas-phase PES peaks are shown below curve *f*.

in Fig. 2, these peaks are distinguishable from the OH features by their different photon-energy dependence. The ability to distinguish between the two possibilities points to the value of having a variable-wavelength photon source (a synchrotron and monochromator) available to do the variable-wavelength UPS studies.

Photon-stimulated desorption

Having identified the species present on the Ti crystal after the H₂O adsorption, we shall now present the results of our other major interest: The study of the energetics and mechanisms of photon-stimulated desorption of ions (PSD).

Direct mass analysis of PSD ions was not possible in these experiments. The usual time-of-flight (TOF) method using the pulsed nature of the synchrotron light source²⁰ cannot be employed at SURF due to the short time intervals between light pulses, ~ 9 nsec. Also, the ion counting rates are too low to attempt to measure the ion flight time by pulsing the sample and gating a grid in front of the detector.²¹

With our present apparatus, we must assume that the mass of the ions desorbed under photon impact is the same as that of those desorbed under electron impact. In general, different ion species desorbed from the same surface have different kinetic-energy distributions.²² We assume if the kinetic-energy distribution observed in PSD is the same as that observed in ESD with low-energy electrons (~ 50 eV), then the ions are the same species. This is not to say that different distributions necessarily mean different species since the same species could desorb from the surface with

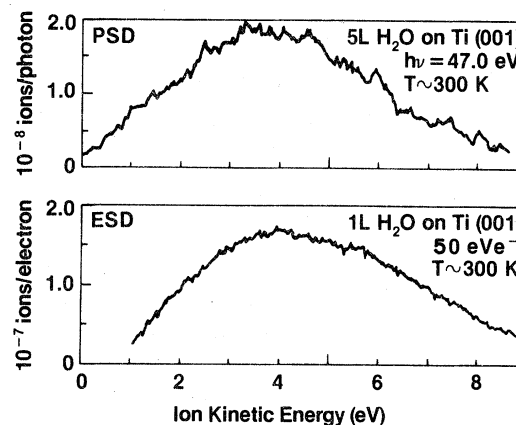


FIG. 4. Ion kinetic-energy distributions compared for PSD and ESD.

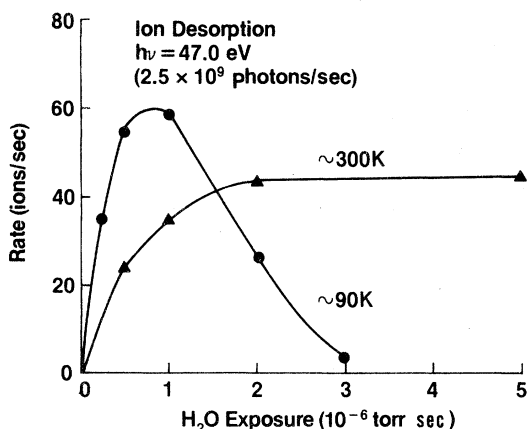


FIG. 5. Ion yield as a function of exposure for water on Ti(001).

two mechanisms or from different states which yield different distributions. The ESD TOF showed the ions desorbed from the H_2O -dosed Ti(001) crystal to be almost exclusively H^+ with contributions from higher-mass ions to be less than 1%. A comparison of ESD and PSD ion kinetic-energy distributions is made in Fig. 4. The near identity in the location of the peaks of the two curves ($\sim 3.8 \text{ eV}$) and in their full width at half-maximum ($\sim 5 \text{ eV}$) leads us to conclude that the same ions (H^+) are being desorbed in both cases. Likewise, the near identity in the ion desorption rates as a function of coverage for PSD and ESD leads to the same conclusion.

Figure 5 shows the PSD ion intensity as a function of exposure for both the room- and low-temperature experiments for a photon energy of 47 eV near the maximum ion H^+ -ion yield. At room temperature, the H^+ intensity steadily increases to

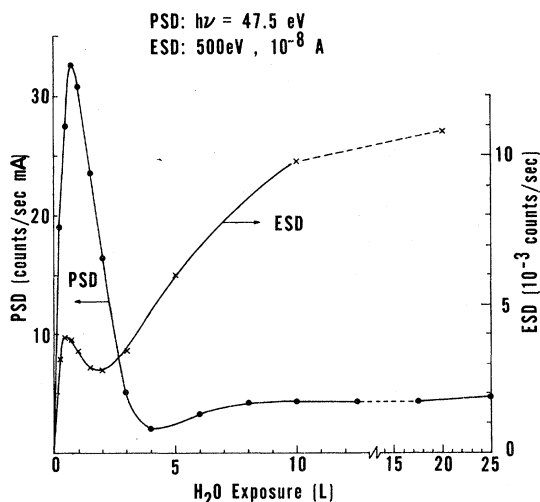


FIG. 6. Comparison of PSD and ESD H^+ ion yield as a function of exposure for water on Ti(001).

saturation at approximately 2 L. At low temperature, the curve rises more steeply and at $\sim 1 \text{ L}$ reaches a maximum which is higher than the intensity of the room-temperature saturation dose. The curve then falls to a low value at 3 L and remains low for higher doses.

The unusual PSD behavior was examined on a second Ti crystal having its surface oriented within 0.5° of the (001) plane, and the results are shown in Fig. 6. For PSD using a photon energy of 47.5 eV, the H^+ ion yield rises initially upon exposure of the surface to H_2O , passes through a sharp maximum at $\sim 0.75 \text{ L}$, and falls as the dose increases. The high H^+ yield at low doses appears to be related to the formation of $\text{OH}(\text{ads})$, and the decrease at high doses is due to the formation of an ice multilayer. The ESD H^+ yield as a function of H_2O exposure is also shown in Fig. 6. As in the PSD case, the H^+ yield rises to a maximum for low H_2O exposure. However, the ESD H^+ yield rises significantly at higher doses, in marked contrast to the PSD yield. It is clear that bombardment of an ice multilayer by 500-eV electrons results in electronic excitations caused by both primary and secondary electrons which lead to appreciable H^+ emission, and that 47-eV photons do *not* cause such excitations. This is consistent with the data of Rosenberg *et al.*⁶ who found that the ion yield versus photon energy for H^+ from amorphous ice was maximum at $\sim 30 \text{ eV}$. The low counting rates for PSD of H^+ from ice in the present work did not permit a precise comparison with the data of Rosenberg *et al.*⁶ but our results are qualitatively consistent.

The H^+ ion yield as a function of photon energy for $\sim 0.5\text{-L}$ H_2O on Ti(001) is shown in Fig. 7. For comparison, the O^+ ion yield from O_2 dosed on this crystal as well as the secondary electron yield from the same crystal are shown.⁹ The PSD data are corrected for monochromator transmission and second-order contributions.²³ The dashed lines indicate regions where there are uncertainties in the amplitudes of the yields due to uncertainties in the second-order corrections.^{23,24} However, the structure and, in particular, the threshold at 25 eV in the H^+ yield curve are not affected by the uncertainties.

The three curves are qualitatively similar above 40 eV, showing a peak at 45 eV and a slow decrease toward higher photon energy. The low-energy region, however, appears quite different for the H^+ yield curve. Its onset is near 25 eV which is $\sim 5 \text{ eV}$ below the onsets for either the O^+ ion yield or the secondary electron yield. Also, the H^+

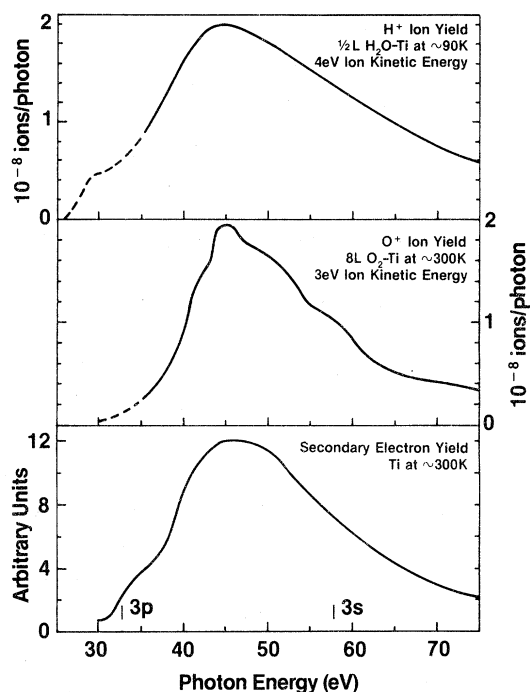


FIG. 7. Ion yield as a function of photon energy for water on Ti(001) (top) compared with that for oxygen on the same substrate (middle) and the secondary electron yield for the clean substrate.

curve shows a second onset at a photon energy of ~ 33 eV near the onset for the Ti $3p$ core-hole excitation,^{9,25} which is marked at the bottom of the figure and which is near the onset of the secondary electron yield curve.

The H^+ -ion yield for low H_2O doses is definitely associated with the presence of OH on the surface. Hydrogen adsorbed on this same crystal, while producing the UPS features ascribed to H as mentioned above, did not produce a measurable PSD ion signal in the (25–75)-eV photon-energy range. Likewise, the H^+ -ion signal from the ice layer in this range of photon energies is almost an order of magnitude lower than the signal from the dissociated H_2O . In addition, the coadsorption of hydrogen with a fractional monolayer of oxygen (oxygen followed by hydrogen as well as vice versa) resulted in H^+ signals smaller by an order of magnitude than those observed here for OH from the dissociated H_2O . We conclude that the H^+ observed in PSD either originates from the OH radical on the surface or is produced from a state of H on the surface which is activated by the presence of OH. In short, our results indicate that the OH must be present on the surface in order to produce the measured H^+ signal.

DISCUSSION

The results of water adsorption on the stepped Ti(001) crystal reveal several interesting phenomena. It appears that water dissociates on this surface to form three species: O, H, and OH. On most other surfaces water adsorbs either molecularly,⁷ forms H and OH (Ref. 2), or dissociates completely⁵ to O and H. This indicates the possibility that the water is adsorbed at two different types of sites on this surface, one producing H and OH, the other H and O. The dissociation of H_2O on Ti films at 300 K was also recently verified by Kandasamy and Surplice.²⁶

The second interesting observation concerns the PSD and ESD ion yield data. Only H^+ is observed in the ESD TOF measurements, with no O^+ or OH^+ . This is contrary to previous results from H_2O adsorption on defect TiO_2 where O^+ , H^+ , and OH^+ were observed.²⁷ Our results are similar to the PSD results from amorphous ice,⁶ in that only H^+ is observed in both experiments. However, the H^+ intensity here appears to be an order of magnitude greater from the OH than from the H_2O covered surface.

The H^+ PSD ion yield curve for OH(ads) shows a threshold at 25 eV which is near the H^+ desorption threshold observed by Knotek from OH on TiO_2 .²⁷ The desorption for photon energies of 25–35 eV may be initiated by the $O2s$ core-hole excitation which has its onset in this energy range. This mechanism is illustrated in the top portion of Fig. 8.

There appears to be little correlation between the ion yield and the photon-energy dependence of the UPS photon yield from the OH-derived spectral features (Fig. 2). Thus, ionization of the one-electron levels with binding energies of ~ 7.4 and 11.4 eV is not responsible for H^+ ion desorption observed here.

The second threshold near 35 eV in the yield curve and the peak at 45 eV suggests that the Ti $3p$ core hole is involved in the desorption at photon energies above 33 eV. This is a bit surprising since the H^+ desorption appears to require the presence of OH on the surface as discussed above. We offer two possible bonding configurations to explain these observations. The first, illustrated in Fig. 8(a), has OH bonded to the Ti substrate through the O. Excitation of the substrate core hole by the photon results in the breaking of the O–H rather than the Ti–OH bond. This would be the first reported example of the desorption of an ion by the excitation of an atom other than the atom to

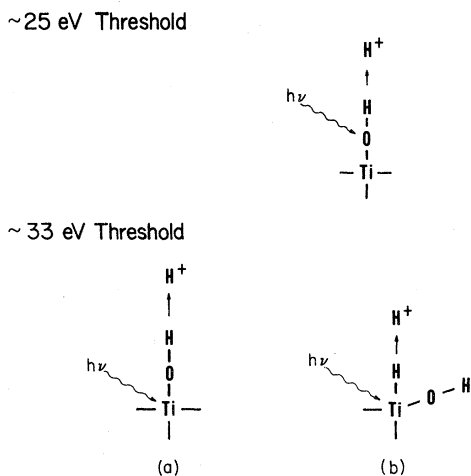


FIG. 8. Possible mechanisms for the desorption of H^+ from water on Ti(001). The 25-eV threshold is associated with the excitation of the O $2s$ core hole. The 33-eV threshold is associated with the excitation of the Ti $3p$ core hole. Since the H^+ desorption is associated with the presence of OH on the surface, the H^+ arises from either (a) the H in the OH, or (b) H attached to a Ti to which an OH is also attached.

which the desorbing ion is bonded. In all other studies of PSD to date, the bond being ruptured is between the excited atom and the desorbing ion. However, it would be surprising if such a process could occur without the desorption of some OH, since OH^+ is seen from H_2O on TiO_2 .²⁷

Figure 8(b) illustrates a second configuration in which some of the OH and H are bonded to the same Ti atom at a low coordination site (step edge). The excitation of the Ti core hole leads to H^+ desorption only if OH is also bonded to the same Ti atom. However, one would expect that O might have the same effect as the OH, i.e., if O and H were bonded to the same Ti atom, H^+ desorption should occur with approximately the same probability. However, the hydrogen and oxygen coadsorption experiments show that $H + O$ on the surface does not yield significant H^+ , arguing against this explanation, though it is possible that O and H do not bond to the same Ti atom as OH and H might.

Recent work by Ramaker²⁸ indicates that different excitations may be responsible for PSD of H^+ from adsorbed OH. He suggests that the threshold at ~ 25 eV is due to a two-hole excitation in the uppermost valence orbitals of adsorbed OH (shakeup plus ionization) and that the higher-energy process, with the peak at 45 eV, is due to ionization of the O $2s$ level.

The increase in H^+ -ion yield with increasing H_2O exposure for exposures < 1 L (Fig. 5) is quite different from the behavior seen for O^+ from Ti(001),⁹ W(111),²⁹ or Nb(001) (Ref. 30) with increasing oxygen exposure. In those cases, low oxygen doses lead to population of binding states with low PSD cross sections. Only when the oxygen approaches or exceeds monolayer coverages is there a high O^+ PSD cross section due to oxygen adsorbed at low coordination sites, step edges, etc. In contrast, molecular adsorption of CO on Ru(001),³¹ Pd(210),³² and Ni(111) (Ref. 33) yields an ESD ion yield which increases directly with exposure at low coverage. This suggests that special sites are not necessary to generate an ESD or PSD active species, but that all sites (terraces as well as step edges) are effective. Thus, the majority of molecular CO adsorbed at low coverage contributes to the ion yield, while only a minority of the adsorbed atomic oxygen contributes.

It appears from Fig. 5 that the H^+ from OH is similar to the case of molecular CO adsorption, in that the H^+ yield is directly proportional to H_2O exposure. If special sites are required for formation of the PSD-active complex, they either have a very high density, and/or the H_2O has a very high mobility at both 90 and 300 K.

Finally, we note that the striking difference between the ESD and PSD H^+ -ion yields from an ice multilayer (Fig. 6) is due to the fact that the 500-eV electron beam causes electronic excitations in ice which are not induced by 47.5-eV photons.

CONCLUSION

To conclude, we summarize our results for water adsorption on a stepped Ti(001) crystal: (i) At 300 K, water dissociates on this surface to form adsorbed O, H, and OH. No molecular H_2O is adsorbed at 300 K. (ii) At 90 K, for water exposures less than 1 L, dissociation also occurs and the same species are formed. For higher H_2O exposures, molecular H_2O is adsorbed, and multilayer H_2O film growth is observed. (iii) PSD and ESD studies at 90 and 300 K reveal the desorption of H^+ ions. A high H^+ signal is associated with the presence of OH on the surface; the PSD signal from the ice multilayer is significantly smaller. (iv) From the photon-energy dependence of the H^+ PSD yield from adsorbed OH, two desorption thresholds are identified suggesting that two different excitation mechanisms produce the H^+ signal.

ACKNOWLEDGMENTS

We wish to thank the staff of the National Bureau of Standards Synchrotron Ultraviolet Radiation Facility for assistance in conducting the experiments and D. Ramaker for valuable discus-

sions. One of us (D.M.H.) wishes to acknowledge support provided by the University of Maryland through the SURF Fellowship Program. This work was supported in part by the Office of Naval Research.

- *Temporary address: Institute of Physical Science and Technology, University of Maryland, College Park, Maryland. Permanent address: Department of Chemistry, State University of New York, Stony Brook, New York 11794.
- †Permanent address: Department of Physics, Linköping University, S-581-83 Linköping, Sweden.
- ¹S. J. Atkinson, C. R. Brundle, and M. W. Roberts, *Discuss. Faraday Soc.* **58**, 62 (1974).
- ²G. B. Fisher and J. L. Gland, *Surf. Sci.* **94**, 446 (1980); G. B. Fisher and B. A. Sexton, *Phys. Rev. Lett.* **44**, 683 (1980).
- ³H. Ibach and S. Lehwald, *Surf. Sci.* **91**, 187 (1980).
- ⁴D. J. Dwyer, G. W. Simmons, and R. P. Wei, *Surf. Sci.* **64**, 617 (1977).
- ⁵C. Benndorf, C. Nobl, M. Rusenberg, and F. Thieme, *Surf. Sci.* **111**, 87 (1981).
- ⁶R. A. Rosenberg, V. Rehn, V. O. Jones, A. K. Green, C. C. Parks, G. Loubriel, and R. H. Stulen, *Chem. Phys. Lett.* **80**, 488 (1981).
- ⁷F. P. Netzer and T. E. Madey, *Phys. Rev. Lett.* **47**, 928 (1981); T. E. Madey and F. P. Netzer, *Surf. Sci.* (in press).
- ⁸P. J. Feibelman, D. R. Hamann, and F. J. Himpsel, *Phys. Rev. B* **22**, 1734 (1980).
- ⁹D. M. Hanson, R. Stockbauer, and T. E. Madey, *Phys. Rev. B* **24**, 5513 (1981).
- ¹⁰D. L. Ederer, B. E. Cole, and J. B. West, *Nucl. Instrum. Methods* **172**, 185 (1980).
- ¹¹A. C. Parr, R. Stockbauer, B. E. Cole, D. L. Ederer, J. L. Dehmer, and J. B. West, *Nucl. Instrum. Methods* **172**, 357 (1980).
- ¹²M. M. Traum and D. P. Woodruff, *J. Vac. Sci. Technol.* **17**, 1202 (1980).
- ¹³E. B. Saloman, *Nucl. Instrum. Methods* **172**, 79 (1980).
- ¹⁴T. E. Madey and J. T. Yates, Jr., *Surf. Sci.* **63**, 203 (1977).
- ¹⁵R. Stockbauer, D. M. Hanson, and T. E. Madey (unpublished).
- ¹⁶L. I. Johansson, A. L. Hagström, A. Platau, and S. E. Karlsson, *Phys. Status Solidi B* **83**, 77 (1977).
- ¹⁷S. Katsumata and D. R. Lloyd, *Chem. Phys. Lett.* **45**, 519 (1977).
- ¹⁸C. R. Brundle and M. W. Roberts, *Surf. Sci.* **38**, 234 (1973).
- ¹⁹D. W. Turner, C. Baker, A. D. Baker, and C. R. Brundle, *Molecular Photoelectron Spectroscopy* (Wiley, New York, 1970), p. 113.
- ²⁰R. Jaeger, J. Stohr, J. Feldhaus, S. Brennan, and D. Menzel, *Phys. Rev. B* **23**, 2102 (1981).
- ²¹J. F. Van der Veen, F. J. Himpsel, D. E. Eastman, and P. J. Heimann, *Solid State Commun.* **36**, 99 (1980).
- ²²T. E. Madey and J. T. Yates, Jr., *J. Vac. Sci. Technol.* **8**, 525 (1971).
- ²³T. E. Madey and R. Stockbauer, in *Methods in Experimental Physics—Surfaces*, edited by R. L. Park and M. G. Lagally (in press).
- ²⁴D. P. Woodruff, P. D. Johnson, M. M. Traum, H. H. Farrell, N. V. Smith, R. L. Benbow, and Z. Hurych, *Surf. Sci.* **104**, 282 (1981).
- ²⁵D. A. Shirley, R. L. Martin, S. P. Kowalczyk, F. R. McFeely, and L. Ley, *Phys. Rev. B* **15**, 544 (1977).
- ²⁶K. Kandasamy and N. A. Surplice, *J. Phys. C* **15**, 1089 (1982).
- ²⁷M. L. Knotek, *Surf. Sci.* **91**, L17 (1980).
- ²⁸D. Ramaker (unpublished).
- ²⁹T. E. Madey, R. Stockbauer, J. F. van der Veen, and D. E. Eastman, *Phys. Rev. Lett.* **45**, 187 (1980).
- ³⁰R. L. Stockbauer, D. M. Hanson, S. A. Flodström, and T. E. Madey (unpublished).
- ³¹T. E. Madey, *Surf. Sci.* **79**, 575 (1979); P. Feulner, H. A. Engelhardt, and D. Menzel, *Appl. Phys.* **15**, 355 (1978).
- ³²T. E. Madey, J. T. Yates, Jr., A. M. Bradshaw, and F. M. Hoffmann, *Surf. Sci.* **89**, 370 (1979).
- ³³F. P. Netzer and T. E. Madey, *J. Chem. Phys.* **76**, 710 (1982).